RESEARCH ARTICLE

Aldehyde and Ketone Hydroboration Mediated by a Heterogeneous Single-Site Molybdenum-Dioxo Catalyst: Scope and Mechanistic Implications

Yiqi Liu,[a] Amol Agarwal,[b] Yosi Kratish,*[a] and Tobin J. Marks*[a]

[a] Y. Liu, Prof. Y. Kratish, Prof. T. J. Marks
Department of Chemistry
Northwestern University
2145 Sheridan Road, Evanston, Illinois 60208 (USA)
E-mail: yosi.kratish@northwestern.edu
t-marks@northwestern.edu

[b] A. Agarwal
Department of Material Science and Engineering
Northwestern University
2145 Sheridan Road, Evanston, Illinois 60208 (USA)

Supporting information for this article is given via a link at the end of the document.

Abstract: Efficient hydroboration of aldehydes and ketones is demonstrated using a single-site MoO_2 catalyst supported on activated carbon. Under mild conditions with low catalytic loadings, the reaction exhibits chemoselectivity towards carbonyl reduction over halides, alkene, alkyne, nitrile, and ester groups, affording high yields of desired products. Furthermore, competition studies between aldehyde and ketone reduction using HBpin and HBcat indicate that HBpin preferably functionalizes aldehydes, while HBcat can functionalize either substrate under specific conditions. Mechanistic studies suggest that the reaction proceeds via the initial formation of a molybdenum-hydride species upon B-H activation and subsequent molybdenum-alkoxide species upon carbonyl activation by the Mo center. The experimental activation energy of 14.3 kcal/mol aligns well with the DFT computed $\Delta H^{\ddagger}$ of 18.7 kcal/mol, further supporting the proposed mechanism. Combined experimental/computational analyses reveal that excess HBpin can possibly deactivate the catalyst. The presence of excess benzaldehyde efficiently mitigates deactivation by HBpin, providing significantly higher catalyst recyclability. Overall, this non-toxic, air- and moisture-stable, active, and selective catalyst demonstrates significant potential for green processes.

Introduction

Carbonyl reduction is a transformation of great importance in synthetic organic chemistry to afford diverse functional alcohols with widespread industrial applications.[1] Conventionally, the reduction of aldehydes and ketones requires stoichiometric amounts of metal hydrides, such as $LiAlH_4$ and $NaBH_4$, and suffers from hazards in handling and low functional group tolerance.[2] Therefore, developing green reduction processes with higher atom efficiency, product selectivity, functional group compatibility, and lower hazard in handling is of significant interest. Over recent decades, catalytic hydroboration with less-aggressive reductants, such as pinacolborane (HBpin) or catecholborane (HBcat), has been employed in the reduction of unsaturated bonds.[3] There have been several reports of metal-free and solvent-free hydroboration of ketones and aldehydes, but they have limitations such as the requirement of high reaction temperatures/long reaction times.[4]

While many homogeneous catalysts have been used for hydroboration,[5] they typically have complex ligands, which require multi-step syntheses, and suffer from air- and moisture-sensitivity and low catalyst recyclability. As a result, they have limited applications in academic and large-scale industrial processes. In contrast to their homogeneous analogues, heterogeneous catalysts offer several attractions, such as higher stability, recyclability, and ease of separation from reaction mixtures.[6] Surprisingly, the use of heterogeneous catalysts for hydroboration processes is relatively unexplored, with only a few reported examples such as Zr,[7] Mn,[8] Co,[5i, 9] Mg,[10] Ti,[11] and Fe[12]. Despite having reasonable catalyst stability and recyclability, some of these catalysts require base or hydride activators, which could potentially compete with metal-catalyzed borylation pathways,[13] while others are bulk nanoparticles with ill-defined surface active sites, which can complicate mechanistic and structure-function clarification. Therefore, developing efficient and straightforward synthetic procedures using well-defined heterogeneous catalysts for future up-scaling is still in its infancy.

Detailed structural understanding is key to connecting structure and activity/selectivity in heterogeneous catalysis and can provide unique insights into unusual fundamental chemistry, mechanistic understanding, and the design of next-generation catalysts. Single-site heterogeneous catalysts (SSHCs) have emerged as an appealing option, bridging the gap between homogeneous and heterogeneous catalysts by providing well-defined active sites on the surface.[14] Typically, molecular precursors are directly grafted onto solid supports to prepare SSHCs.[15] Motivated by the earth-abundance, low-toxicity, and versatile catalytic activities of homogeneous Mo-oxo species and the desirable properties of activated carbon (high surface area and low cost), recent efforts in this laboratory have involved the design and evolution of single-site Mo-dioxo catalysts supported

on activated carbon, AC/MoO_2, and exploring the scope of their catalytic properties.[16] The single-site nature of this catalytic system has been well-characterized by IR, XPS, SMART-EM, EXAFS/XANES, and DFT methodologies, suggesting well-dispersed Mo(VI)-dioxo species with two Mo=O bonds and two Mo-O bonds.[17] This catalyst is highly active for a variety of transformations, including ester and alcohol activation,[16, 18] as well as coupled oxidation-reduction reactions.[19] Moreover, it is competent for the reductive coupling of carbonyls with silanes.[20] In this process, the catalyst is capable of activating Si-H bonds and demonstrates high selectivity towards symmetric ether products, with silyl ethers and desilylated alcohols as the by-products. Therefore, we were intrigued by the possibility that this catalyst might also be competent for activating B-H across Mo=O bonds, to catalyze hydroboration processes. To our knowledge there have been no reports of carbonyl hydroboration mediated by heterogeneous molybdenum complexes or single-site metal-oxo species.

In this contribution, we describe the efficient and selective hydroboration of aldehydes and ketones catalyzed by AC/MoO_2 (Tables 1-2). This system operates under mild conditions and employs low loading of the single-site MoO_2 catalyst that is both air- and moisture-stable, providing high yields of the desired products with good functional group tolerance. An in-depth understanding of the surface species and mechanistic pathways is obtained with a combined experimental (EXAFS, XPS, NMR) and computational DFT study. Overall, this contribution showcases the efficient hydroboration of aldehydes and ketones mediated by a robust, structurally and mechanistically well-defined AC/MoO_2 catalytic system.

Results and Discussion

An initial study focused on the AC/MoO_2-catalyzed hydroboration of benzaldehyde with HBpin. Investigations of catalyst loading and reaction temperature were conducted (Table 1, entries 1-3). In the presence of 5 mol% of AC/MoO_2, 98% yield of the borylated product is achieved in 24 h at room temperature. However, decreasing the catalytic loading to 2 mol% affords only a 71% yield in 24 h. Increasing the reaction temperature to 60 °C leads to >99% yield of the borylated product after 3 h. Note that negligible yields are observed when the activated carbon support alone or no catalyst is used (Table 1, entries 4-5), highlighting the importance of the catalytically active MoO_2 sites. When bulk MoO_3 is used under the same conditions, the borylated product is obtained in a modest 50% yield (Table 1, entry 6), significantly lower than with AC/MoO_2, emphasizing the importance of isolated single-site MoO_2 species. Table 1 summarizes the full scope of aldehydes investigated in this report. Note that negligible HBpin decomposition is observed under the current reaction conditions, providing the desired borylation products selectively.[21] Besides benzaldehyde, more sterically hindered 2,4,6-trimethyl-benzaldehyde is also efficiently reduced by this system (Table 1, entry 7). Electron-rich *p*-tolualdehyde and 2-naphthaldehyde, and electron-poor 4-chlorobenzaldehyde and 4-bromobenzaldehyde are similarly reduced, affording 91-99% yields of the desired products (Table 1, entries 8-11). The catalyst also retains good chemoselectivity towards C=O reduction in the presence of alkene and alkyne, yielding selectively 84-99% of the desired borylated products (Table 1, entries 12-13). The heterocyclic substrate, 3-thiophenecarboxaldehyde, affords >99% yield of the corresponding borylated product in 1 h (Table 1, entry 14). The aliphatic substrate, cyclohexanecarboxaldehyde, is also efficiently reduced by the system, affording 97% of the desired product (Table 1, entry 15). The effect of substrate lone pairs which might compete with C=O coordination was next assessed with 4-methoxybenzaldehyde and 4-cyanobenzaldehyde. Note that these substrates require 24 h and 48 h, respectively, to provide quantitative yields of the borylated products (Table 1, entries 16-17). This reduced rate likely reflects competing coordination of the substrate oxygen and nitrogen lone pairs to the Lewis acidic Mo catalyst.[22] Previous research has shown that strong electron-donating substrates such as pyridine can poison the AC/MoO_2 catalytic center.[17b]

Encouraged by the excellent activity and selectivity of the aldehyde hydroboration reactions, we then extended the carbonyl scope examination to ketones. Note that under the optimized reaction condition used in Table 1, only 8% yield of the acetophenone borylated product is observed after 24 h (Table 2, entry 1). Therefore, alternative reducing agents with higher reactivity were examined. HBcat is a stronger Lewis acid and thus is considered to be a more potent reducing agent than HBpin.[23] Gratifyingly, in the presence of 2 mol% of AC/MoO_2, full conversion of acetophenone is achieved within 12 h at 60˚C using HBcat as the reducing agent, affording 98% yield of the borylated product (Table 2, entry 2). In addition, negligible HBcat decomposition is observed under the current reaction conditions.[24] When no catalyst is used, only 16% yield is obtained in 12 h (Table 2, entry 3), demonstrating the importance of catalytically active MoO_2 sites. Note that 56% yield of the borylated product is observed when bulk MoO_3 is used (Table 2, entry 4). Table 2 summarizes the full scope of ketones investigated. Similar to aldehydes, electron-rich 4-methylacetophenone and 2-acetonaphthone are efficiently reduced by this system, affording 77% and 95% yield of the desired product, respectively (Table 2, entries 5-6). Notably, some alkene side-products are observed with these two substrates, possibly due to hydrolysis of the borylated products followed by alcohol dehydration to afford alkenes. Note that previous research has shown that AC/MoO_2 is competent to catalyze alcohol dehydration.[18c] Moreover, electron-poor 4-chloroacetophenone, 4-bromoacetophenone, and 4-(trifluoromethyl)acetophenone are also efficiently reduced by this system, exhibiting halide tolerance and minimal electronic effects and affording 95-99% yield of the borylated products (Table 2, entries 7-9). The catalyst also retains chemoselectivity towards C=O reduction in the presence of esters and nitriles, affording 95% and 88% of the borylated product, respectively (Table 2, entries 10-11). Reaction rates are generally slower with sterically demanding ketones, such as dicyclohexyl ketone, isobutyrophenone, and cyclohexyl phenyl ketone, requiring 24-48 h to afford quantitative yields of the desired products (Table 2, entries 12-14).

Table 1. AC/MoO_2-catalyzed aldehyde hydroboration scope.[a]

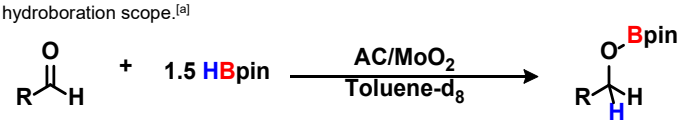

Entry	Substrate	Product	Catalyst loading (mol%)	Temperature (°C)	Time (h)	Yield (%)
1	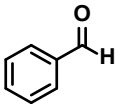	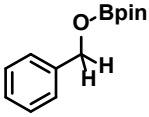	5	25	24	98
2			2	25	24	71
3			2	60	3	>99
4			Activated carbon	60	3	5
5			-	60	3	5
6			MoO_3	60	3	50
7	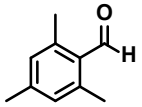	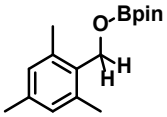	2	60	3	97
8	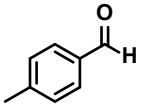	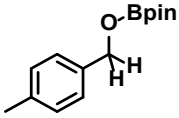	2	60	3	>99
9	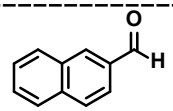	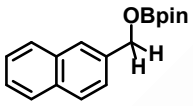	2	60	24	91
10	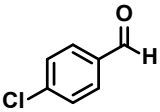	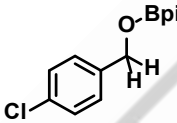	2	60	3	96
11	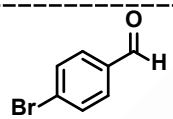	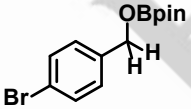	2	60	24	95
12	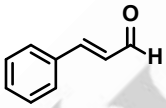	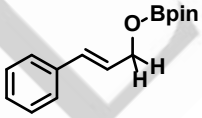	2	60	3	>99
13	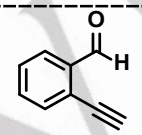	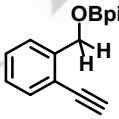	2	60	6	84
14	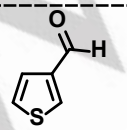	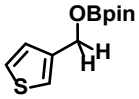	2	60	1	>99
15	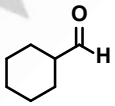	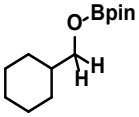	2	60	6	97
16	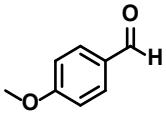	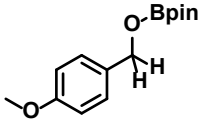	2	60	24	>99

17	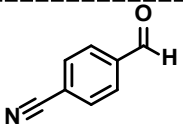	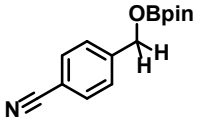	2	60	48	74

[a] Conditions unless otherwise specified: 0.4 mmol of substrate, 0.6 mmol of HBpin, 2 mol% of Mo (33.4 mg of 2.3 wt% AC/MoO_2), 0.14 mmol of mesitylene, 2 mL of toluene-d_8, 500 rpm, 60 °C, under Ar. Yields were determined by ^{1}H NMR spectroscopy using mesitylene as an internal standard.

Table 2. AC/MoO_2-catalyzed ketone hydroboration scope.[a]

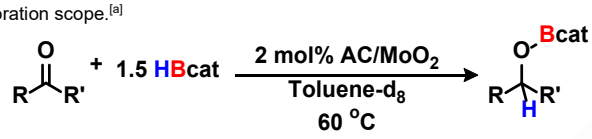

Entry	Substrate	Product	Catalyst loading (mol%)	Time (h)	Yield (%)
1[b]	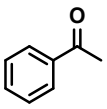	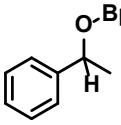	2	24	8
2	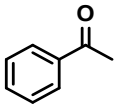	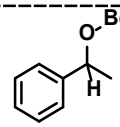	2	12	98
3			-	12	16
4			MoO_3	12	56
5	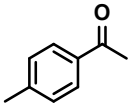	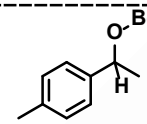	2	12	77[c]
6	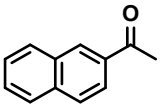	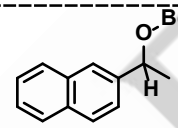	2	12	95[c]
7	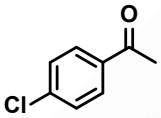	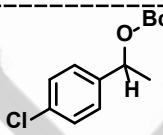	2	12	98
8	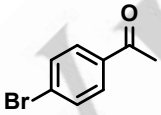	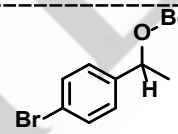	2	12	95
9	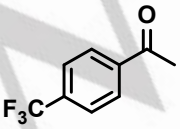	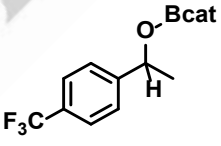	2	12	>99
10	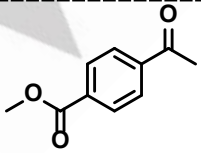	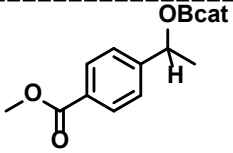	2	12	95
11	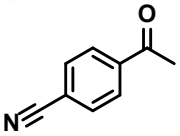	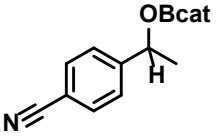	2	12	88

12	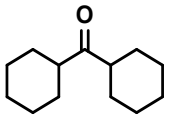	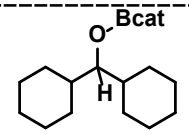	2	24	87
13	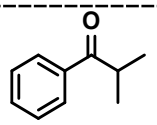	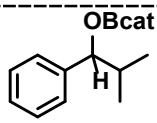	2	48	94
14	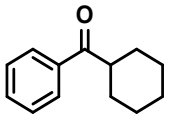	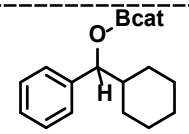	2	48	92

[a] Conditions unless otherwise specified: 0.4 mmol of substrate, 0.6 mmol of HBcat, 2 mol% of Mo (33.4 mg of 2.3 wt% AC/MoO_2), 0.14 mmol of mesitylene, 2 mL of toluene-d_8, 500 rpm, 60 °C, under Ar. Yields were determined by ^{1}H NMR spectroscopy using mesitylene as an internal standard. [b] HBpin was used as the reducing agent. [c] Alkene by-products were observed alongside borylated main products.

To better understand the selectivity of the different reductants, competition studies between ketone and aldehyde were next conducted in the presence of HBpin and HBcat (Table 3). When equimolar benzaldehyde and acetophenone are allowed to compete for 1.5 equiv. of HBpin, preference for aldehyde hydroboration is observed, yielding 93% of the hydroborated aldehyde (**1**) with only 10% of the hydroborated ketone (**2**) (Table 3, entry 1).[3a, 25] As expected, when excess HBpin is used, full conversion of benzaldehyde is achieved after 12 h, affording a 97% yield of **1**. However, even after 72 h, only 32% yield of **2** is observed (Table 3, entry 2), demonstrating that HBpin exhibits high selectivity for aldehyde over ketone hydroboration. When equimolar benzaldehyde and acetophenone are allowed to compete for 1.5 equiv. of HBcat, preference for aldehyde hydroboration is still observed, affording >99% yield of benzaldehyde functionalized product (**1**) and only 19% of acetophenone functionalized product (**2**) (Table 3, entry 3). When excess HBcat is used (3 equiv.), both borylated products are obtained in >99% yield after 30 h, indicating HBcat's capability to fully borylate aldehyde and ketone (Table 3, entry 4).

As previously noted, high recyclability is a great advantage of heterogeneous catalysts. Therefore, recyclability experiments were performed for acetophenone hydroboration with HBcat. When a fresh catalyst is used, the borylated product is obtained in 55% yield after 1 h and in 74% yield after 3 h at 60 ˚C (Figure 1a), while full acetophenone conversion and quantitative yield of the borylated product can be achieved in 12 h. The catalyst is then separated from the reaction mixture by filtration, washed with hexane, and dried under a vacuum overnight. Next, a fresh batch of acetophenone and HBcat is added, and the reaction mixture is allowed to react at 60 ˚C. Unexpectedly, the observed yield in the next run is 75% after 1 h, higher than the 55% yield obtained after 1 h using a fresh catalyst. Moreover, a quantitative yield can be obtained in 3 h (Figure 1a). This possibly reflects the neutralization of catalytically inactive sites, which compete for substrate binding during the first catalytic run and hinder catalysis. Interestingly, the catalyst maintains its high catalytic activity for at least 2 subsequent runs, affording quantitative conversions and yields within 3 h.

Table 3. Competitive aldehyde/ketone hydroboration selectivity study.[a]

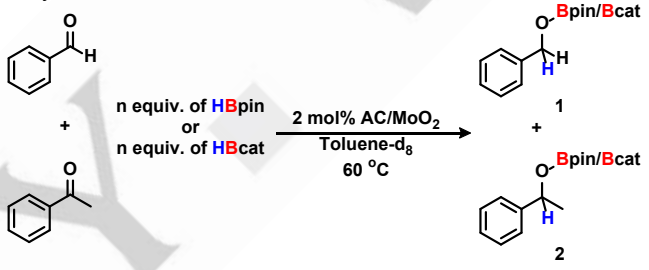

Entry	Reductant	Equiv.	Time (h)	Yield of 1 (%)	Yield of 2 (%)
1	HBpin	1.5	3	93	10
2	HBpin	3	3	97	18
			12	>99	20
			72	>99	32
3	HBcat	1.5	3	>99	19
4	HBcat	3	3	>99	44
			12	>99	86
			30	>99	>99

[a] Conditions: 0.4 mmol of benzaldehyde, 0.4 mmol of acetophenone, 0.6 mmol (1.5 equiv.) or 1.2 mmol (3 equiv.) of HBpin or HBcat, 2 mol% of Mo (33.4 mg of 2.3 wt% AC/MoO_2), 0.14 mmol of mesitylene (internal standard), 2 mL of toluene-d_8, 500 rpm, 60 °C, under Ar. Yields were determined by ^{1}H NMR spectroscopy using mesitylene as an internal standard.

Next, recyclability experiments were performed for benzaldehyde hydroboration with HBpin. When 2 mol% loading of the fresh catalyst is used, 96% yield of the borylated product is obtained after 1 h (Figure 1b). Surprisingly, when the catalyst is recycled and used in the next run, only 73% yield is obtained after 1 h, while quantitative yield (99%) can still be achieved after 3 h. When the catalyst is reused for 2 more runs, even lower yields are obtained. In the third run, 70% yield is observed after 3 h,

whereas only 33% yield is obtained after 3 h in the fourth run. Overall, decreasing yields are observed when recycled catalysts are used, suggesting that the catalyst has been deactivated during the reaction.

To explore the presence of possible deactivators, a control experiment was performed in which AC/MoO_2 was allowed to react with HBpin at 60 °C overnight, after which benzaldehyde was added to the reaction mixture. This reaction affords 18% yield of the borylated product after 1 h and 50% yield after 3 h, which is far slower than when HBpin and benzaldehyde were added together (Table 1, entry 3, >99% yield), suggesting that HBpin possibly deactivates the catalyst. According to XPS analysis, the fresh catalyst has a single Mo $3d_{5/2}$ ionization at 232.8 eV, indicating the presence of bound Mo^{VI} species, whereas the recycled catalyst, which is collected from aldehyde hydroboration reaction with HBpin, has Mo $3d_{5/2}$ ionizations at 232.0 eV and 230.3 eV, assignable to Mo^{VI} and Mo^{IV} species, respectively (Figure S1a-b).[26] This result is also in good agreement with XAS analysis. According to the XANES data, the recycled catalyst has a lower Mo K-edge energy than the fresh catalyst, suggesting that the Mo species has been reduced in the recycled catalyst (Figure S2). In addition, the EXAFS fittings reveal that the double bond character has decreased in the recycled catalyst, consistent with the reduction of the surface sites (Figure S3). Thus, the XAS data align well with XPS results, suggesting the formation of Mo^{IV} species in the catalyst deactivation pathway.

In an attempt to mitigate the HBpin deactivating effects, hydroboration runs were carried out using a 10-fold molar excess of benzaldehyde with respect to HBpin, while the catalyst loading remained at 2 mol% (Figure 1c). While the reaction rate still falls slightly after each run, the use of excess benzaldehyde shows that the catalyst deactivation can be avoided by reducing the HBpin-catalyst contact time. Note that, unlike the results shown in Figure 1b, all recyclability runs in the current case achieve quantitative yields after 3 h (Figure 1c). According to XPS analysis, the Mo species in the recycled catalyst largely retains the +6

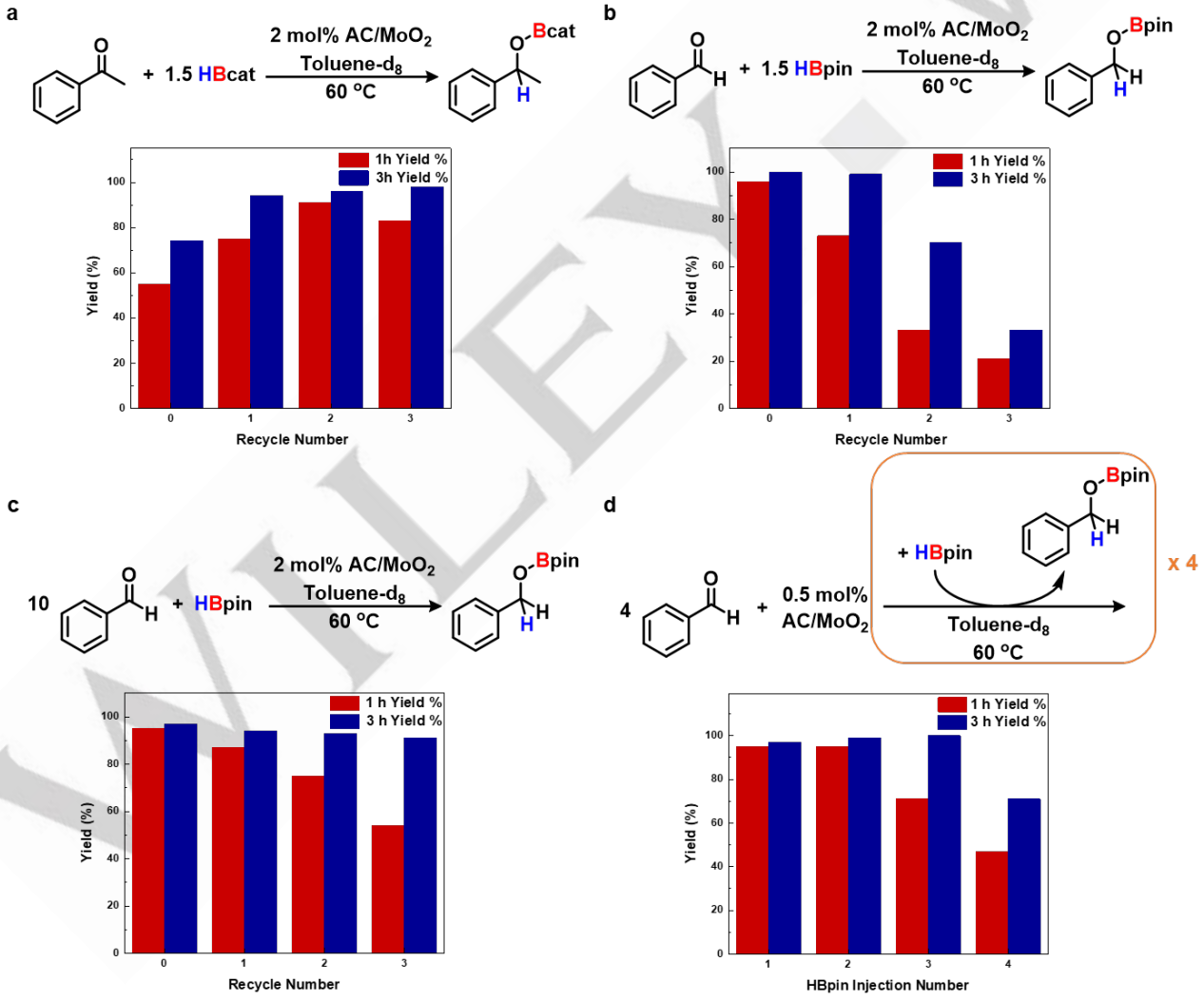

Figure 1. Recycling experiments. (a) AC/MoO_2 catalyzed hydroboration of acetophenone with HBcat (excess). (b) AC/MoO_2 catalyzed hydroboration of benzaldehyde with HBpin (excess). (c) AC/MoO_2 catalyzed hydroboration of benzaldehyde (excess) with HBpin. (d) AC/MoO_2 catalyzed hydroboration of benzaldehyde with multiple injections of HBpin.

oxidation state without observable Mo^{IV} species (Figure S1c). Moreover, hydroboration runs were carried out when excess benzaldehyde was allowed to react during slow continuous injection of HBpin in the presence of 0.5 mol% AC/MoO_2 (Figure 1d). In the first run, 4 equiv. of benzaldehyde is allowed to react with 1 equiv. of HBpin, affording full HBpin consumption and quantitative yield of the borylated product in 1 h. Then, another equiv. of HBpin is added to the reaction mixture and allowed to react with the remaining benzaldehyde, still affording 95% yield of the desired product in 1 h. Slow catalyst deactivation is observed only after the third HBpin injection, possibly due to the decreasing concentration of the remaining benzaldehyde to mitigate catalyst deactivation by HBpin (Figure 1d). Overall, these data demonstrate that the presence of excess benzaldehyde alleviates catalyst deactivation and enhances catalyst recyclability.

Next, a DFT analysis was carried out to better understand the catalytic hydroboration mechanism as well as the catalyst deactivation pathway. To reduce computational costs, the four methyl groups of HBpin were substituted with hydrogen substituents (**HBpin***). DFT calculations were performed at the CAM-B3LYP/Def2-SVP//CAM-B3LYP-D3/Def2-TZVP level of theory using ORCA 4.1.0 package.[27] The proposed catalytic cycle is elaborated in Scheme 1a, with key transition states shown in Scheme 1b.

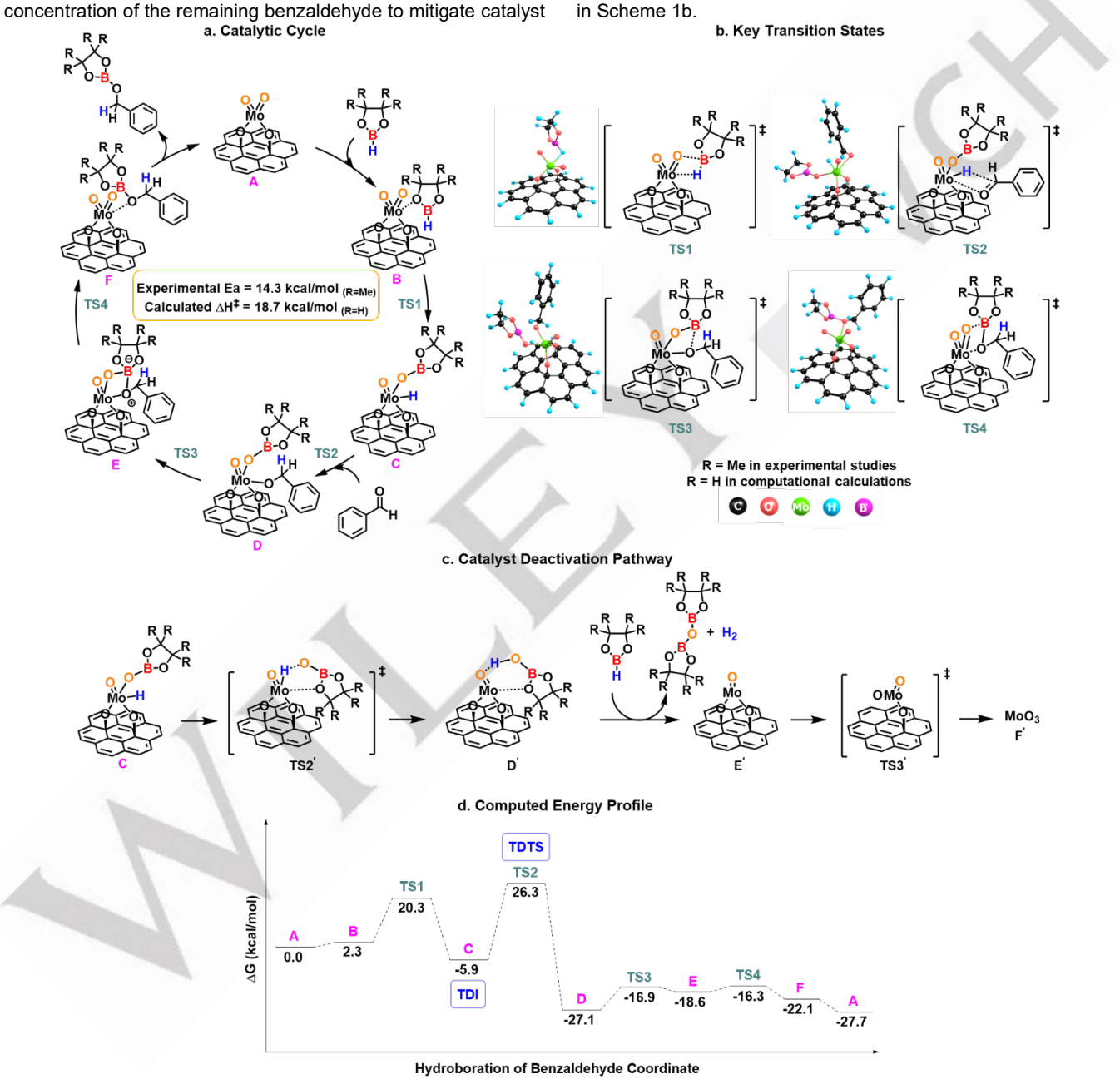

Scheme 1. DFT analysis of benzaldehyde hydroboration with HBpin catalyzed by AC/MoO_2. (a) Computed catalytic cycle. (b) Key transition states. (c) Catalyst deactivation pathway. (d) Computed enthalpy profile in kcal/mol. TDI = turnover-determining intermediate, TDTS = turnover-determining transition state.

The calculated Gibbs free energy profile for the catalytic cycle is shown in Scheme 1d. In the first step, **HBpin*** coordinates to the Mo center (**A**) via its glycol oxygen atom (Scheme 1a, species **B**). In the next step, the B-H bond is activated across the Mo=O bond via a concerted four-membered ring transition state (Scheme 1a, **TS1**) to afford the Mo-hydride species **C**. This step has an energetic barrier of 18 kcal/mol and is exergonic by –8.2 kcal/mol. In the next step, the aldehyde carbonyl oxygen coordinates to the Mo center, and the Mo-H bond is added to the C=O bond to yield Mo-alkoxide species **D**. This step is the rate-determining step of the catalytic cycle with an energy barrier of 32.2 kcal/mol and a $\Delta H^{\ddagger}$ of 18.7 kcal/mol (**TS2**). The computed $\Delta H^{\ddagger}$ is in excellent agreement with the experimental activation energy of 14.3 kcal/mol obtained from the Arrhenius plot, further supporting the proposed mechanism (Figure S4). Note that in the case of acetophenone, the calculated rate-determining transition state is higher by ~1 kcal/mol, in good agreement with the observed slower reaction kinetics (Table 2, entry 1) and the high selectivity for aldehyde hydroboration in the competition study as discussed above (Table 3). In addition, when HBcat is used instead of HBpin, the calculated barrier falls by 4.3 kcal/mol and 4.5 kcal/mol for benzaldehyde and acetophenone (Scheme S1), respectively, in agreement with the observed rate increase when HBcat is used as the reducing agent. Next, the Mo-alkoxide moiety can nucleophilically attack the electropositive boron ligand to yield zwitterionic intermediate **E**. Note that this intramolecular step has a low energy barrier **(TS3**, $\Delta G^{\ddagger}$ = 10.2 kcal/mol). Next, species **E** can undergo another low energy B-O bond dissociation step (**TS4**, $\Delta G^{\ddagger}$ = 2.3 kcal/mol) to yield species **F**. Finally, spontaneous (ΔG = -5.6 kcal/mol) desorption of the borylated aldehyde product occurs to regenerate the dioxo-molybdenum catalyst (Scheme 1a, species **A**). A similar mechanism was proposed for homogeneous Mo-oxo catalysts.[28]

A plausible catalyst deactivation pathway is shown in Scheme 1c with the calculated energy profile detailed in Scheme S2. Interestingly, the addition of **HBpin*** to AC/MoO_2 can reduce its oxidative state from Mo(VI) to Mo(IV) by abstracting one oxo ligand, yielding Mo(IV) intermediate **E'** and **HOBpin***. Thus, in the first stage of the reduction pathway, intermediate **C** undergoes a reductive elimination step (**TS2'**), during which the Mo-O and Mo-H bonds are cleaved while an O-H bond is formed, yielding a -**HOBpin*** still coordinated to the Mo center (Scheme 1c, **D'**). This step has a computed energy barrier of 31.9 kcal/mol, similar to that of **TS2** in the catalytic cycle ($\Delta G^{\ddagger}$ = 32.2 kcal/mol), indicating that -**HOBpin*** formation competes with the hydroboration pathway (Scheme S2). The bound -**HOBpin*** species can then undergo reaction with another equiv. of **HBpin***, yielding **(Bpin*)$_2$O** and H_2,[29] and Mo(IV) species **E'** in a strongly exergonic step of ΔG = -9.2 kcal/mol (Scheme S2). According to the calculation, **E'** can readily undergo **MoO_3** elimination from the carbon support in a strongly exergonic step (ΔG = -91.2 kcal/mol) in a practically barrier-less process (**TS3'**, 3.0 kcal/mol). As noted previously, as-purchased MoO_3 is a much less active catalyst for benzaldehyde hydroboration with HBpin, affording only 50% yield in 3 h, which explains the lower reaction rate observed with recycled catalysts. To further validate the deactivation pathway experimentally, AC/MoO_2 was reacted with excess HBpin at 60 °C for 3 h. As expected, H_2 and a quantitative formation of **(Bpin*)$_2$O** are observed by NMR (Figure S5-6), supporting the proposed pathway. According to XPS analysis, the HBpin-treated catalyst has Mo $3d_{5/2}$ ionizations at 232.2 eV and 230.1 eV, representing Mo^{VI} and Mo^{IV} species, respectively (Figure S7), supporting the proposed deactivation pathway in which the Mo(VI) center is reduced to Mo(IV). This is similar to the XPS data observed in the recycled deactivated catalyst shown in Figure 1b (Figure S1).

Conclusions

We report a robust, earth-abundant, and easily separated single-site heterogeneous MoO_2 catalyst for efficient hydroboration of a large scope of aldehydes and ketones with HBpin and HBcat. The functional group tolerance has been demonstrated by high chemoselectivity towards the reduction of carbonyl substrates while leaving C=C, C≡C, halide, nitrile, and ester functionalities untouched. Competition studies demonstrate that HBpin preferably borylates aldehydes over ketones. An in-depth understanding of the catalytic cycle and catalyst deactivation pathway has been achieved with a combined experimental and DFT computational analysis. The presence of excess aldehyde can mitigate HBpin poisoning effect, providing higher catalyst recyclability. Overall, AC/MoO_2 exhibits promise as an alternative to homogeneous catalysts used in hydroboration reactions, as it is structurally and mechanistically well-defined and provides insights into future structure-function studies and the design of next-generation single-site catalysts.

Acknowledgements

Financial support was provided by the U.S. Department of Energy, Office of Science, Office of Basic Energy Sciences under Award Number DOE DE-FG02-03ER15457 to the Institute for Catalysis in Energy Processes (ICEP) at Northwestern University. This work made use of IMSERC facilities at Northwestern University, which have received support from Soft and Hybrid Nanotechnology Experimental (SHyNE) Resource (NSF ECCS-2025633), Int. Institute of Nanotechnology, and Northwestern University. This work made use of Northwestern University QBIC generously supported by NASA Ames Research Center Grant NNA04CC36G. We thank Dr. Jake Rothbaum and Dr. Qingheng Lai at Northwestern University, who generously provided insights and expertise that assisted the research.

Keywords: heterogeneous catalysis • molybdenum • single-site catalysts • hydroboration • mechanistic studies

[1] J. Magano, J. R. Dunetz, *Organic Process Research & Development* **2012**, *16*, 1156-1184.

[2] aH. C. Brown, S. Narasimhan, *J. Org. Chem.* **1982**, *47*, 1604-1606; bN. G. Gaylord, *J. Chem. Educ.* **1957**, *34*, 367.

[3] aC. C. Chong, R. Kinjo, *ACS Catal.* **2015**, *5*, 3238-3259; bM. L. Shegavi, S. K. Bose, *Catal. Sci. Technol.* **2019**, *9*, 3307-3336; cS. J. Geier, C. M. Vogels, J. A. Melanson, S. A. Westcott, *Chem. Soc. Rev.* **2022**, *51*, 8877-8922.

[4] aH. Stachowiak, J. Kaźmierczak, K. Kuciński, G. Hreczycho, *Green Chem.* **2018**, *20*, 1738-1742; bW. Wang, M. Luo, W. Yao, M. Ma, S. A. Pullarkat, L. Xu, P.-H. Leung, *New J. Chem.* **2019**, *43*, 10744-10749; cS. Sau, M. Pramanik, A. Bal, P. Mal, *Chem. Rec.* **2022**, *22*, e202100208.

[5] aK. Makarov, A. Kaushansky, M. S. Eisen, *ACS Catal.* **2022**, *12*, 273-284; bS. Mahato, P. Rawal, A. K. Devadkar, M. Joshi, A. Roy Choudhury, B. Biswas, P. Gupta, T. K. Panda, *Org. Biomol. Chem.* **2022**, *20*, 1103-1111; cA. M. Poitras, L. K. Oliemuller, G. P. Hatzis, C. M. Thomas, *Organometallics* **2021**, *40*, 1025-1031; dM. Magre, B. Maity, A. Falconnet, L. Cavallo, M. Rueping, *Angew. Chem., Int. Ed.* **2019**, *58*, 7025-7029; eD. H. Ma, A. K. Jaladi, J. H. Lee, T. S. Kim, W. K. Shin, H. Hwang, D. K. An, *ACS Omega* **2019**, *4*, 15893-15903; fA. Harinath, J. Bhattacharjee, T. K. Panda, *Adv. Synth. Catal.* **2019**, *361*, 850-857; gC. J. Barger, A. Motta, V. L. Weidner, T. L. Lohr, T. J. Marks, *ACS Catal.* **2019**, *9*, 9015-9024; hV. L. Weidner, C. J. Barger, M. Delferro, T. L. Lohr, T. J. Marks, *ACS Catal.* **2017**, *7*, 1244-1247; iG. Zhang, H. Zeng, J. Wu, Z. Yin, S. Zheng, J. C. Fettinger, *Angew. Chem., Int. Ed.* **2016**, *55*, 14369-14372; jS. Bagherzadeh, N. P. Mankad, *ChemComm* **2016**, *52*, 3844-3846.

[6] J. D. A. Pelletier, J.-M. Basset, *Acc. Chem. Res.* **2016**, *49*, 664-677.

[7] N. Eedugurala, Z. Wang, U. Chaudhary, N. Nelson, K. Kandel, T. Kobayashi, I. I. Slowing, M. Pruski, A. D. Sadow, *ACS Catal.* **2015**, *5*, 7399.

[8] G. Zhang, H. Zeng, S. Li, J. Johnson, Z. Mo, M. C. Neary, S. Zheng, *Dalton Trans.* **2020**, *49*, 2610-2615.

[9] aK. Manna, P. Ji, Z. Lin, F. X. Greene, A. Urban, N. C. Thacker, W. Lin, *Nat. Commun.* **2016**, *7*, 12610; bJ. Wu, H. Zeng, J. Cheng, S. Zheng, J. A. Golen, D. R. Manke, G. Zhang, *J. Org. Chem* **2018**, *83*, 9442-9448.

[10] K. Manna, P. Ji, F. X. Greene, W. Lin, *J. Am. Chem. Soc.* **2016**, *138*, 7488-7491.

[11] Z. Huang, D. Liu, J. Camacho-Bunquin, G. Zhang, D. Yang, J. M. López-Encarnación, Y. Xu, M. S. Ferrandon, J. Niklas, O. G. Poluektov, J. Jellinek, A. Lei, E. E. Bunel, M. Delferro, *Organometallics* **2017**, *36*, 3921-3930.

[12] aL. Li, E. Liu, J. Cheng, G. Zhang, *Dalton Trans.* **2018**, *47*, 9579-9584; bM. L. Shegavi, A. Baishya, K. Geetharani, S. K. Bose, *Org. Chem. Front.* **2018**, *5*, 3520-3525; cN. Antil, N. Akhtar, R. Newar, W. Begum, A. Kumar, M. Chauhan, K. Manna, *ACS Catal.* **2021**, *11*, 10450-10459; dR. Newar, N. Akhtar, N. Antil, A. Kumar, S. Shukla, W. Begum, K. Manna, *Angew. Chem. Int. Ed.* **2021**, *60*, 10964-10970.

[13] I. P. Query, P. A. Squier, E. M. Larson, N. A. Isley, T. B. Clark, *J. Org. Chem.* **2011**, *76*, 6452-6456.

[14] aT. D. Tilley, *J. Mol. Catal. A Chem.* **2002**, *182-183*, 17-24; bJ. M. Thomas, R. Raja, D. W. Lewis, *Angew. Chem. Int. Ed.* **2005**, *44*, 6456-6482; cS. L. Wegener, T. J. Marks, P. C. Stair, *Acc. Chem. Res.* **2012**, *45*, 206-214.

[15] aN. M. Schweitzer, B. Hu, U. Das, H. Kim, J. Greeley, L. A. Curtiss, P. C. Stair, J. T. Miller, A. S. Hock, *ACS Catal.* **2014**, *4*, 1091-1098; bN. Merle, F. Le Quéméner, Y. Bouhoute, K. C. Szeto, A. De Mallmann, S. Barman, M. K. Samantaray, L. Delevoye, R. M. Gauvin, M. Taoufik, J.-M. Basset, *J. Am. Chem. Soc.* **2017**, *139*, 2144-2147; cT. Fu, Y. Wang, A. Wernbacher, R. Schlögl, A. Trunschke, *ACS Catal.* **2019**, *9*, 4875-4886; dM. Pucino, F. Zhai, C. P. Gordon, D. Mance, A. H. Hoveyda, R. R. Schrock, C. Copéret, *Angew. Chem. Int. Ed.* **2019**, *58*, 11816-11819.

[16] A. R. Mouat, T. L. Lohr, E. C. Wegener, J. T. Miller, M. Delferro, P. C. Stair, T. J. Marks, *ACS Catal.* **2016**, *6*, 6762-6769.

[17] aY. Kratish, T. Nakamuro, Y. Liu, J. Li, I. Tomotsuka, K. Harano, E. Nakamura, T. J. Marks, *BCSJ* **2020**, *94*, 427-432; bY. Liu, J. Li, A. Das, H. Kim, L. O. Jones, Q. Ma, M. J. Bedzyk, G. C. Schatz, Y. Kratish, T. J. Marks, *J. Am. Chem. Soc.* **2021**, *143*, 21532-21540; cY. Liu, A. Agarwal, Y. Kratish, T. J. Marks, *Angew. Chem. Int. Ed.* **2023**, *62*, e202304221.

[18] aT. L. Lohr, A. R. Mouat, N. M. Schweitzer, P. C. Stair, M. Delferro, T. J. Marks, *Energy Environ. Sci.* **2017**, *10*, 1558-1562; bY. Kratish, J. Li, S. Liu, Y. Gao, T. J. Marks, *Angew. Chem. Int. Ed.* **2020**, *59*, 19857-19861; cJ. Li, A. Das, Q. Ma, M. J. Bedzyk, Y. Kratish, T. J. Marks, *ACS Catal.* **2022**, *12*, 1247-1257.

[19] J. Li, S. Liu, T. L. Lohr, T. J. Marks, *ChemCatChem* **2019**, *11*, 4139-4146.

[20] S. Liu, J. Li, T. Jurca, P. C. Stair, T. L. Lohr, T. J. Marks, *Catal. Sci. Technol.* **2017**, *7*, 2165-2169.

[21] aA. D. Bage, T. A. Hunt, S. P. Thomas, *Org. Lett.* **2020**, *22*, 4107-4112; bM. Uzelac, K. Yuan, M. J. Ingleson, *Organometallics* **2020**, *39*, 1332-1338; cK. Nicholson, T. Langer, S. P. Thomas, *Org. Lett.* **2021**, *23*, 2498-2504; dA. D. Bage, K. Nicholson, T. A. Hunt, T. Langer, S. P. Thomas, *Synth.* **2022**, *55*, 62-74; eD. R. Willcox, S. P. Thomas, *Beilstein J. Org. Chem.* **2023**, *19*, 325-348.

[22] S. F. Rach, F. E. Kühn, *Chem. Rev.* **2009**, *109*, 2061-2080.

[23] aA. Caise, D. Jones, E. L. Kolychev, J. Hicks, J. M. Goicoechea, S. Aldridge, *Eur. J. Chem.* **2018**, *24*, 13624-13635; bT. J. Hadlington, C. E. Kefalidis, L. Maron, C. Jones, *ACS Catal.* **2017**, *7*, 1853-1859.

[24] aS. Harder, J. Spielmann, *J. Organomet. Chem.* **2012**, *698*, 7-14; bA. D. Bage, K. Nicholson, T. A. Hunt, T. Langer, S. P. Thomas, *ACS Catal.* **2020**, *10*, 13479-13486.

[25] S. Lau, C. B. Provis-Evans, A. P. James, R. L. Webster, *Dalton Trans.* **2021**, *50*, 10696-10700.

[26] aY. Huang, J. Ge, J. Hu, J. Zhang, J. Hao, Y. Wei, *Adv. Energy Mater.* **2018**, *8*, 1701601; bM. Hou, X. Teng, J. Wang, Y. Liu, L. Guo, L. Ji, C. Cheng, Z. Chen, *Nanoscale* **2018**, *10*, 14594-14599.

[27] aT. Yanai, D. P. Tew, N. C. Handy, *Chem. Phys. Lett.* **2004**, *393*, 51-57; bF. Neese, *Wiley Interdiscip. Rev. Comput. Mol. Sci.* **2012**, *2*, 73-78.

[28] aL. Huang, J. Wang, X. Wei, H. Wei, *Catal. Sci. Technol.* **2015**, *5*, 3259-3269; bM. Drees, T. Strassner, *Inorg. Chem.* **2007**, *46*, 10850-10859.

[29] D. Wu, R. Wang, Y. Li, R. Ganguly, H. Hirao, R. Kinjo, *Chem* **2017**, *3*, 134-151.

Entry for the Table of Contents

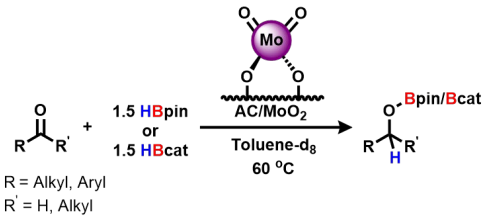

- ✓ Low catalyst loading
- ✓ Selective over C=C, C≡C, halide, nitrile, and ester functionalities
- ✓ In-depth investigation of catalytic cycle and deactivation pathway

The efficient hydroboration of a wide variety of aldehydes and ketones using a single-site carbon-supported MoO_2 catalyst is reported. The reaction exhibits chemoselectivity towards carbonyl reduction over C=C, C≡C, halide, nitrile, and ester functionalities. In-depth analyses of reaction mechanism and catalyst deactivation pathway have been supported by combined experimental and computational studies.